

## Fabrication of nanoelectrodes and nanojunction hydrogen sensor

Syed Mubeen,<sup>1</sup> Bongyoung Yoo,<sup>2</sup> and Nosang V. Myung<sup>1,a)</sup>

<sup>1</sup>*Chemical and Environmental Engineering and Center for Nanoscale Science and Engineering, University of California-Riverside, Riverside, California 92521, USA*

<sup>2</sup>*Division of Materials and Chemical Engineering, Hanyang University, Ansan 426-791, Republic of Korea*

(Received 3 July 2008; accepted 29 August 2008; published online 1 October 2008)

A simple method to fabricate nanoelectrodes with controllable gap was demonstrated by local electrical melting of nickel nanowire. The width of nanogap was tuned by diameter of nanowire and the gap distance was controlled by voltage sweep rate. These nanoelectrodes were then electrochemically backfilled with palladium to fabricate hydrogen nanojunction sensor. Sensors showed excellent sensing performance (dynamic range from 0.1% to 4% H<sub>2</sub> and <1 min response time for H<sub>2</sub> concentration >2%) at room temperature. Our method of electrochemically backfilling a nanogap opens up a possibility to create various nanojunction devices in a cost-effective manner. © 2008 American Institute of Physics. [DOI: 10.1063/1.2993337]

Nanojunction devices have attracted a great deal of attention both fundamentally and application wise as it allows studying the transport phenomena at molecular/nanoscale scale.<sup>1</sup> Two main challenges in realizing molecular/nanoelectronics are fabricating high density nanoelectrodes with controllable gaps in a cost-effective manner and creating stable electrical contact. Different methods have been employed to address the issue such as mechanical break junctions,<sup>2,3</sup> electromigration,<sup>4,5</sup> shallow-angled evaporations,<sup>6</sup> self-assembled monolayers,<sup>7</sup> *e*-beam lithography methods,<sup>8</sup> electrodeposition,<sup>9,10</sup> and dip pen lithography.<sup>11</sup> However, creating a stable electrical contact between the molecules/nanomaterials to these nanoelectrodes still remains a great challenge. Most commonly used methodologies include modifying the nanoelectrodes using covalent<sup>12</sup> and noncovalent chemistry,<sup>13</sup> electrostatic trapping of molecules between the electrodes,<sup>14</sup> self-assembly,<sup>15</sup> and thermal evaporation of the desired material.<sup>16</sup> Though these methods have been able to contact molecules, getting good control and stable contact is still yet to be realized.

Here we report a robust, controllable, and cost-effective approach of fabricating stable nanojunction devices by electrodeposition materials between nanogap electrodes. The fabrication of nanojunction sensor starts by spatially positioning the ferromagnetic nanowires using magnetic field alignment technique followed by electrically melting them by sweeping voltages at high scan rates. Then pulsed plating was performed for depositing the desired material between these nanoelectrodes. Since the current density is highly localized at the tip of the nanowire, it is expected that the desired material locally deposits between nanoelectrodes forming a nanojunction. In addition, since the electrodeposition can be monitored in real time, the deposition could be immediately terminated once an electrical contact has been made allowing good control over nanojunction fabrication.

Conventional materials used for fabricating nanoelectrodes are generally metal electrodes such as lithographically defined gold electrodes,<sup>8</sup> gold nanowires,<sup>5</sup> carbon nanotubes,<sup>13</sup> etc. We utilized ferromagnetic nanowires for

fabricating nanoelectrodes, as they can be spatially positioned on the desired sites by using magnetic alignment technique.<sup>17</sup> We synthesized nickel nanowires (200 nm in diameter and 10 μm long) using template-directed electrodeposition, an approach pioneered by Martin.<sup>18</sup> The deposition procedure and deposition conditions are mentioned elsewhere.<sup>17</sup> After electrodeposition, the nickel nanowires were suspended in isopropanol by mechanical removal of gold seed layer followed by selective etching of the alumina scaffolds using concentrated NaOH (5 M) for 8 h at 60 °C.<sup>19</sup> The resulting high density nanowire suspension was diluted up to 1000-fold for subsequent alignment between the gold electrodes using a weak magnetic field. In order to magnetically assemble ferromagnetic nanowires only in the gap between the electrodes, one of the gold electrodes was electrodeposited with a ferromagnetic material (i.e., cobalt), thus the nanowires are assembled only between the electrodes and not on the SiO<sub>2</sub> substrate increasing the usage efficiency of nanowires.<sup>20</sup> The number of bridged nanowires was controlled by adjusting the concentration of the nanowire suspension. After magnetic alignment of the nanowires, the interconnect was subjected to annealing in a reduced environment (i.e., 5% hydrogen+95% nitrogen) for 1 h at 300 °C. Annealing reduced any oxide layer formed around the nanowire and also lowered the contact resistance between the nanowire and the contact pad.

In order to create nanogap electrodes, we used an electrical breakdown method. In a typical electrical breakdown experiment, the bias voltage across a thin metallic film or wire is increased up to the point where the wire breaks or snaps. It is a well studied phenomenon and is taken into serious consideration while designing interconnects in integrated circuits. Two important phenomena occur during the voltage ramp: electromigration and joule heating. With increasing current densities over a period of time, the conducting atoms of the metal start to move in the same direction of the electron flow, resulting in a current induced diffusion of atoms, which then leads to a void in the current path. This process is called electromigration.<sup>21</sup> The other consequence to the electrical transport, joule heating, creates thermomechanical stress as a result of different thermal expansion coefficients between the wire and the substrate during heating of the wire, and is found to have a maximum at the center of

<sup>a)</sup>Author to whom correspondence should be addressed. Electronic mail: myung@engr.ucr.edu. Tel.: 1-951-827-7710. FAX: 1-951-827-5696.

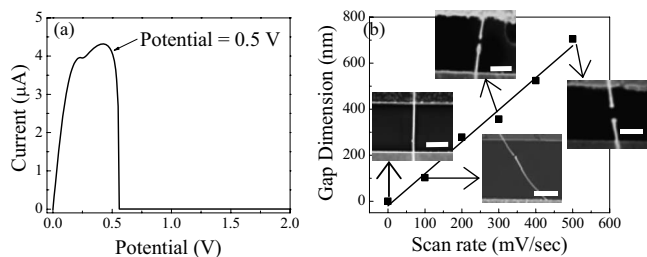


FIG. 1. Nanogap formation. (a) Potential sweeping process resulting in electrical breaking of wire. (b) Dependence of the gap distance between nanowire electrodes on the voltage scan rate. Inset: SEM images of nanoelectrodes at different scan rates. Scale bars represented  $2 \mu\text{m}$ .

the wire for uniform nanowires.<sup>22</sup> Both these processes are well studied and depend on different variables such as size, shape, thermal coefficient of the material, scan and material diffusion rates, etc. For our studies, we fabricated nanogaps by sweeping voltages at a constant scan rate and measuring the current until it drops to zero [Fig. 1(a)]. We repeated the same experiment for different scan rates from 10 to 500 mV/s. During the voltage scan, the current initially increased linearly with an increase in applied voltage. As the applied voltage increased further, the slope of the  $I$ - $V$  curve decreased indicating nonuniform movement of electrons because of a high degree of collision. At such high currents, the stress created by thermal means (joule heating) is much higher than stress created due to interdiffusion of atoms (electromigration),<sup>22</sup> resulting in abrupt failure at the center of the wire and formation of the nanogap [Fig. 1(b)]. We observed that at low scan rates (10 mV/s) the time required to break a nanowire was too long, and the gap was either formed at the cathode end of the electrode, or the wire got completely melted. Though the failure at the cathode end might be dominated by electromigration rather than joule heating resulting in tensile stress failure of the material,<sup>22</sup> the reason for complete burning of the wire observed for some cases is still under investigation. As the scan rate is increased ( $>100$  mV/s), we observed clear breaking of the nanowire at the midsection as joule heating was the dominant factor at higher scan rates,<sup>21</sup> and the gap width increased with increasing scan rate. At very high scan rates, the nanowire broke catastrophically, making nanogap fabrication difficult to control. Hence, in subsequent studies we selected a scan rate of 100 mV/s, which gave us a reproducible gap size of approximately 100 nm.

After determining the conditions to reproducibly fabricate nanoelectrodes with a controlled gap length, a nanojunction hydrogen sensor was fabricated by backfilling the gap with electrodeposited palladium. A schematic procedure for backfilling is shown in Fig. 2(b). A  $1 \mu\text{l}$  drop in palladium electrolyte (the electrolyte composition is mentioned elsewhere)<sup>23</sup> was placed over the nanogap using a micropipette. When an electrical potential is applied, the material grows from one end of the nanowire, serving as a cathode, to the other end of the wire, serving as an anode, until the nanogap is bridged. Electrodeposition of palladium was carried out under pulse plating (the peak current was  $-10$  nA, on-time and off-time were 2 and 5 s, respectively) with a two electrode configuration using nickel nanowires as working and counter electrodes. The nickel nanowire on the cobalt pad served as the cathode and the nanowire on the gold pad served as the anode. Pulsed plating was selected over direct

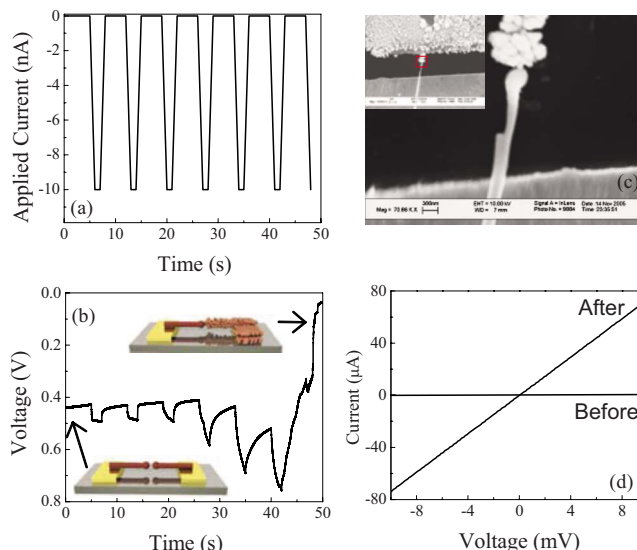


FIG. 2. (Color online) Backfilling of the gap by electrodeposition: (a) applied pulsed current waveform, (b) potential response, (c) SEM image showing nanogap backfilled with Pd, and (d) before and after  $I$ - $V$  characteristics of the backfilled device.

current plating to minimize the trapping of the accompanied hydrogen gas on the surface of the electrode during reduction in palladium ions. Figure 2(b) shows a cathode potential response with respect to time during the electrodeposition of palladium for constant current applied ( $-10$  nA). Upon application of a  $-10$  nA current pulse [Fig. 2(a)], the potential of the cathode dropped steeply and increased to a more negative value from the open circuit potential of  $-0.42$  V to about  $-0.54$  V. With an increase in number of deposition pulses the potential gradually increased to  $-0.78$  V and finally dropped to zero when a contact was made [Fig. 2(b)]. This abrupt drop in potential is due to the flow of current through the more conducting palladium nanocontact as opposed to lower solution-phase conductance, indicating complete backfilling with palladium. Because of the high electric field between the tips of the nanowires, the deposition was initiated from the tip of the nanowires serving as cathode toward the anode when a constant current was applied. Figure 2(c) clearly shows that palladium was completely filled in the nanogap with 10 nm as the contact dimension as observed under SEM. Electrical measurements on devices when cut and backfilled are shown in Fig. 2(d). The gap distance was approximately 100 nm. As expected, the unfilled nanogap shows open circuit, whereas filled nanogap shows linear  $I$ - $V$ , indicating a formation of metallic conduction pathway across the gap.

Palladium nanojunction sensor was then tested for hydrogen sensing at room temperature. It is well known that palladium has high hydrogen solubility,<sup>24</sup> and thus is a material of choice as the active element for hydrogen sensors or as a hydrogen filter. In the presence of hydrogen, hydrogen dissociates into palladium forming palladium hydride ( $\text{PdH}_x$ ), where the content of dissolved hydrogen depends on temperature and partial pressure of hydrogen. On transformation to palladium hydride, the resistance increases above that of pure palladium. This change in its electrical resistance from Pd to  $\text{PdH}_x$  is used as the basis for our hydrogen sensing experiments.

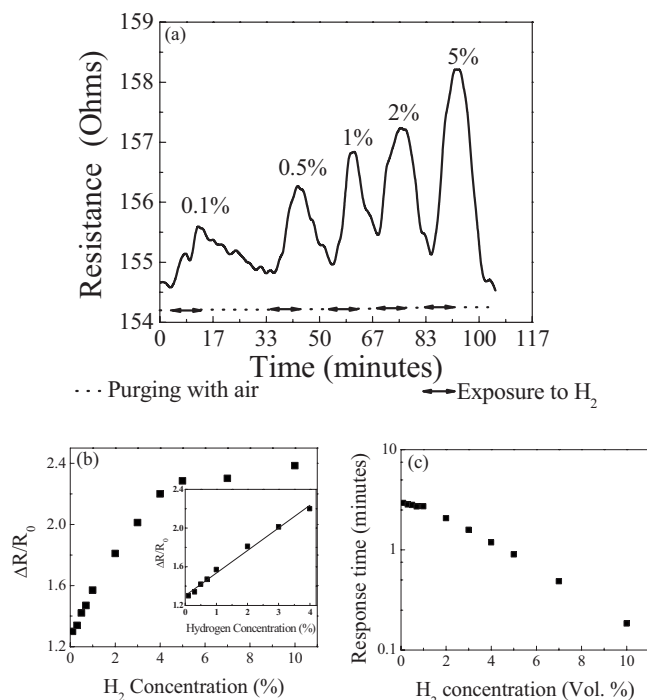


FIG. 3. Hydrogen sensing performance of palladium nanojunction sensor at room temperature. (a) The resistance change with respect to time upon exposure to different concentrations of hydrogen. (b) The sensitivity and (c) response time of sensor as a function of hydrogen concentration.

Before sensing, the devices were mounted onto an independently addressable microband electrodes and wire bonded. The sensor assembly and apparatus is described in detail in our prior works.<sup>25</sup> All experiments were conducted with hydrogen (purity: 99.99%) diluted in argon (purity: 99.998%) at a gas flow of 200 SCCM (SCCM denotes cubic centimeter per minute at STP). All measurements were conducted in a range of hydrogen concentration from 0.1% to 10%. Each sample was primarily exposed to dry argon gas to obtain a baseline followed by a desired percentage of hydrogen gas. After reaching a saturated value, pure argon was reflowed to recover the baseline of the sample. A typical sensing response to hydrogen is shown in Fig. 3(a). Upon exposure to hydrogen gas, the sensor promptly responded with an increase in its initial resistance value, where the saturated resistance has depended on the concentration of hydrogen. Figures 3(b) and 3(c) show the sensor performance and response time of the device for different concentrations of hydrogen, respectively. Sensitivity ( $S$ ) was defined as the percentage of resistance change over baseline resistance, and response time was defined as the time needed for the sensor to reach 90% of the total change for a given concentration of hydrogen. Our nanojunction fabricated sensors showed a good linear sensor performance from 0.1% to 4% with a sensitivity of 0.23 per H<sub>2</sub> concentration in percent. The response time was from tens of seconds at high hydrogen concentration (5%–10%) to 170 s for 0.1%. Our sensor performance and response time are comparable and faster than the ultrathin palladium film based sensors<sup>26</sup> and single palladium based hydrogen sensor operating at room temperature.<sup>27</sup>

In summary, we have demonstrated a simple method to fabricate nanoelectrodes and nanojunction hydrogen sensors.

A detection limit as low as 1000 ppm at room temperature has been demonstrated using these palladium nanojunction hydrogen sensors. Since the desired material is electrodeposited directly between the nanoelectrodes, robust electrical connection with the integrated circuit can be assured, which is important for nanodevices. Our method can also create individually addressable high density nanoelectrodes by site-specific magnetic assembly of multiple nanowires on prefabricated electrodes followed by electrically breaking them in parallel. Furthermore, this method has the potential to further electrochemically grow a quantum dot of semiconductor or any conjugated polymer just by simply changing the electroplating solution and using it for further analysis.

This material is based on research sponsored by the National Institute of Environmental Health Sciences under Grant No. U01ES016026 and the Defense Microelectronics Activity (DMEA) under Agreement No. DOD/DMEA-CNN H94003-06-20604. The United States government is authorized to reproduce and distribute reprints for government purposes, notwithstanding any copyright notation thereon.

- <sup>1</sup>V. P. Menon and C. R. Martin, *Anal. Chem.* **67**, 1920 (1995).
- <sup>2</sup>M. A. Reed, C. Zhou, C. J. Muller, T. P. Burgin, and J. M. Tour, *Science* **278**, 252 (1997).
- <sup>3</sup>H. Park, J. Park, A. K. L. Lim, E. H. Anderson, A. P. Alivisatos, and P. L. McEuen, *Nature (London)* **407**, 57 (2000).
- <sup>4</sup>S. I. Khondaker and Z. Yao, *Appl. Phys. Lett.* **81**, 4613 (2002).
- <sup>5</sup>Y. Selzer, M. A. Cabassi, T. S. Mayer, and D. L. Allara, *J. Am. Chem. Soc.* **126**, 4052 (2004).
- <sup>6</sup>J. Lefebvre, M. Radosavljevic, and A. T. Johnson, *Appl. Phys. Lett.* **76**, 3828 (2000).
- <sup>7</sup>F. R. F. Fan, Y. X. Yao, L. T. Cai, L. Cheng, J. M. Tour, and A. J. Bard, *J. Am. Chem. Soc.* **126**, 4035 (2004).
- <sup>8</sup>K. Liu, Ph. Avouris, J. Bucchnano, R. Martel, S. Sun, and J. Michl, *Appl. Phys. Lett.* **80**, 865 (2002).
- <sup>9</sup>A. F. Morpurgo, C. M. Marcus, and D. B. Robinson, *Appl. Phys. Lett.* **74**, 2084 (1999).
- <sup>10</sup>C. Z. Li, H. X. He, and N. J. Tao, *Appl. Phys. Lett.* **77**, 3995 (2000).
- <sup>11</sup>H. Zhang, S. W. Chung, and C. A. Mirkin, *Nano Lett.* **3**, 43 (2003).
- <sup>12</sup>A. C. Whalley, M. L. Steigerwald, X. Guo, and C. Nuckolls, *J. Am. Chem. Soc.* **129**, 12590 (2007).
- <sup>13</sup>X. Guo, A. Whalley, J. E. Klare, L. Huang, S. O'Brien, M. Steigerwald, and C. Nuckolls, *Nano Lett.* **7**, 1119 (2007).
- <sup>14</sup>A. Bezryadin, C. Dekker, and G. Schmid, *Appl. Phys. Lett.* **71**, 1273 (1997).
- <sup>15</sup>W. Hu, H. Nakashima, K. Furukawa, Y. Kashimura, K. Ajito, and K. Torimitsu, *Appl. Phys. Lett.* **85**, 115 (2004).
- <sup>16</sup>I. Yagi, K. Tsukagoshi, E. Watanabe, and Y. Aoyagi, *Microelectron. Eng.* **73–74**, 675 (2004).
- <sup>17</sup>C. M. Hangarter and N. V. Myung, *Chem. Mater.* **17**, 1320 (2005).
- <sup>18</sup>C. R. Martin, *Science* **266**, 1961 (1994).
- <sup>19</sup>B. Y. Yoo, Y. Rheem, W. P. Beyermann, and N. V. Myung, *Nanotechnology* **17**, 2512 (2006).
- <sup>20</sup>Y. Rheem, B. Y. Yoo, W. P. Beyermann, and N. V. Myung, *Nanotechnology* **18**, 125204 (2007).
- <sup>21</sup>M. L. Trouwborst, S. J. van der Molen, and B. J. van Wees, *J. Appl. Phys.* **99**, 114316 (2006).
- <sup>22</sup>F. O. Hadeed and C. Durkan, *Appl. Phys. Lett.* **91**, 123120 (2007).
- <sup>23</sup>J. Lee, A. A. Wang, Y. Rheem, B. Yoo, A. Mulchandani, W. Chen, and N. V. Myung, *Electroanalysis* **19**, 2287 (2007).
- <sup>24</sup>F. A. Lewis, *The Palladium Hydrogen System* (Academic, New York, 1967).
- <sup>25</sup>S. Mubeen, T. Zhang, B. Y. Yoo, M. Deshusses, and N. V. Myung, *J. Phys. Chem. C* **111**, 6321 (2007).
- <sup>26</sup>O. Dankert and A. Pundt, *Appl. Phys. Lett.* **81**, 1618 (2002).
- <sup>27</sup>Y. Im, C. Lee, R. P. Vasquez, M. A. Bangar, N. V. Myung, E. J. Menke, R. M. Penner, and M. Yun, *Small* **2**, 356 (2006).